

Anelastic media: wave propagation near vertical incidence

P.F. Daley

ABSTRACT

Some of what is presented here was addressed in an earlier work (Daley, 2003). However, as a result of recent papers in the geophysical literature it was determined that this topic should be revisited and specific problems, detailed in the next section, investigated in a numerical manner. When introducing anelasticity into synthetic seismogram computations, selecting a method for accomplishing this while at the same time not introducing non-physical (causality) artefacts into the synthetics is a requisite. This must be done within a mathematical framework without initiating questions as to, among other things, its accuracy, applicability and theoretical correctness. The SEG reprint series (1981), which contains a number of papers on anelastic theory applied to seismic problems. After a significant amount of numerical testing and consultation with other texts and papers related to this matter and with several academic and industry researchers, the theory presented by Futterman (1962) was deemed to be the most useful and accurate when used together with the high frequency geometrical optics solution method of computing synthetic traces. An assumption used in his discussion of seismic wave propagation in a viscoelastic medium is that $Q > 30$. (After numerical experimentation, a minimum value of Q be such that $Q > 30$ might be more realistic)

Although the problem considered here is fairly simplistic, an earlier version of some of the computer code used here is part of a software package, which as of 2008 was still in use in an industry processing package.

BASIC THEORY

The equations of particle motion for an anelastic medium derived by Boltzman are the basis for the theory on which the software used here has been written. A full theoretical development of this problem will not be pursued in this work as it is meant to be only a basic numerical introduction to the topic that is better served by presenting some results rather than a sequence of fairly mathematically intense derivations. To further keep matters as simple as possible only normal incidence will be considered so that the saddle point at all frequencies, which are required to cover the spectrum of the source pulse in the frequency domain, is zero. In the more general non-zero offset case, the saddle point must be computed at each required frequency point for each ray comprising the synthetic trace and is a generally complex quantity, not laying on the real axis in the \mathbf{p} (slowness) plane, but rather in the first quadrant with a time dependence of $e^{-i\omega t}$.

The anelastic equivalents of the elastic medium parameters are assumed to be time dependent and as a consequence, due to the complexity of even a simple problem type, a transformation to the frequency domain is made and most computations are carried out in that domain. This allows for significant latitude in specifying the physical mechanisms that result in a medium being anelastic. The attenuating mechanism discussed in Futterman (1962) assumes that at some reference circular frequency, $\omega_R = 2\pi f_R$ a

reference attenuation factor, $Q_R = Q(\omega_R)$, and reference P – wave velocity, $V(\omega_R)$, are known. These quantities are real valued. At some other frequency, ω , the values of $Q(\omega)$ and $V(\omega)$ are given by the approximations presented by Futterman (1962) as

$$Q(\omega) = Q(\omega_R) \left[1.0 - \frac{1.0}{\pi Q(\omega_R)} \ln \left(\frac{\omega}{\omega_R} \right) \right] \quad (1)$$

and

$$V(\omega) = V(\omega_R) \frac{Q(\omega_R)}{Q(\omega)}. \quad (2)$$

The two values $Q(\omega)$ and $V(\omega)$ obtained above are also real. Anelasticity or attenuation is introduced into a medium through a complex velocity obtained by an analysis of the attenuating mechanism, which as previously stated may be found in Futterman's (1962) paper. His high frequency expression for this complex velocity in terms of the real parameters $Q(\omega)$ and $V(\omega)$ is

$$\frac{1}{C(\omega)} \approx \frac{1}{V(\omega)} \left[1 + \frac{i}{2Q(\omega)} \right] \left\{ \frac{1}{C^2(\omega)} = \frac{1}{V^2(\omega)} \left[1 + \frac{i}{Q(\omega)} \right] \right\}. \quad (3)$$

It should be noted that density is taken to be a real quantity throughout.

The velocity defined by equation (3) is that which is used in the computation of the complex “traveltimes”, geometrical spreading and reflection and transmission coefficients.

In the general case of incidence due to a point source at the surface of a medium composed of plane parallel layers the function to be minimized to determine the saddle point for primary P ray propagation through J layers from the source to a receiver located at the surface is given by

$$f(p) = rp + \sum_{j=1}^J 2h_j \xi_j = \tau_{\text{Re}} + i\tau_{\text{Im}} \quad \text{at } p = p_0 \quad (4)$$

where h_j is the thickness of the j^{th} and the radical ξ_j is defined as

$$\xi_j = (C_j^{-2}(\omega) - p^2)^{1/2} \quad (5)$$

and τ_{Re} and τ_{Im} are the real and positive components of the complex travel time for a given ray. (Actually, the travel time if the ray (τ_{Re}) and a damping factor (τ_{Im}) so that the solution is of the form $A \exp[i\omega\tau_{\text{Im}} - \omega\tau_{\text{Re}}]$ for some complex amplitude A , which is a function of the geometrical spreading.)

At the saddle point $f(p)/dp|_{p=p_0} = 0$ and the geometrical spreading is proportional to

$$d^2f(p)/dp^2|_{p=p_0} = -\sum_{n=1}^N 2h_j / [C_j^2(\omega)\xi_j] \Big|_{p=p_0} \quad (6)$$

If the reflection coefficient is initially taken as a modification of those for a solid/solid interface as in Aki and Richards (1980), it follows that the incident angle dependent reflection coefficient at an interface between two anelastic acoustic media may be generalized to have the form

$$R_{PP}(p) = \frac{\rho_j C_j^2 \xi_j - \rho_{j+1} C_{j+1}^2 \xi_{j+1}}{\rho_j C_j^2 \xi_j + \rho_{j+1} C_{j+1}^2 \xi_{j+1}} \quad (7)$$

where ρ_j is density. In the near vertical incident region equation (7) is a reasonable approximation to the elastodynamic case and, in fact, is exact at normal incidence.

Consider the special case of this reflection coefficient at normal incidence. It will be assumed that at the interface between the j^{th} and $(j+1)^{th}$ layers that the only quantity that varies across the interface is the quality factor, Q . Further, Q_j will be chosen such that the j^{th} layer is elastic, i.e., $Q_j \rightarrow \infty$. The value of Q_{j+1} will be allowed to vary. After some simple algebra, the following result is obtained

$$R_{PP}(p)|_{p=0} = \frac{-i/2Q_{j+1}}{2+i/2Q_{j+1}} = -\frac{i}{4Q_{j+1}(1+i/4Q_{j+1})} \quad (8)$$

The expressions for the modulus and phase of this complex quantity are given by

$$\left|R_{PP}(p)|_{p=0}\right| = \frac{1}{4Q_{j+1}} \frac{1}{(1+1/16Q_{j+1}^2)^{1/2}} \approx \frac{1}{4Q_{j+1}} \quad (9)$$

and

$$\arg[R_{PP}(p)|_{p=0}] = \tan^{-1}(4Q_{j+1}) \quad (10)$$

respectively.

Returning to the more general case it may be seen that in the limit as $p \rightarrow 0$ ($r \rightarrow 0$) then $\xi_n \rightarrow 1/C_n(\omega)$, so that in the normal incidence acoustic case (Brekhovskikh, 1980)

$$R_{pp}(0) = \frac{\rho_j C_j - \rho_{j+1} C_{j+1}}{\rho_j C_j + \rho_{j+1} C_{j+1}} = \frac{I_j - I_{j+1}}{I_j + I_{j+1}} \quad (11)$$

Thus for the problem considered here, at the j -th interface $R_{pp}(0)$ is a function of the complex velocity impedances, $I_n(\omega) = \rho_n C_n(\omega)$ ($n = j, j+1$). The geometrical spreading is similar to the elastic case with the exception that complex quantities are used rather than the real values which result in the elastic case.

NUMERICAL RESULTS

It may first be useful to look at the amplitude versus angle (AVA) case using the acoustic reflection coefficient given in equation (7). Results, amplitude and phase versus incident angle, are presented in Figures (1) and (2) for two cases. The first is a standard problem where the parameters are different in both the upper (incident) and lower media – Figure (1) and the upper medium is assumed to be elastic ($Q_j \rightarrow \infty$) while Q_{j+1} has the values 10, 30, 100 and $Q_{j+1} \rightarrow \infty$ (elastic) in the lower medium. In the second case, all parameters are the same in both media, with the exception of Q_{j+1} . As in the previous case the upper medium is chosen to be elastic. It should be mentioned that Q in both layers is assumed to be frequency independent for this numerical experiment. All required parameters are specified in the figure captions.

Normal incidence synthetic traces computed for a simple model composed of 8 layers over a halfspace are presented next. Actually, it is a four layered model which is repeated twice. This is a common practice in testing certain software packages to ascertain the accuracy of the results computed as there should be an observable relationship between the first and second occurrences of a layer with the same viscoelastic parameters. Only one layer in each of the two sequences is viscoelastic. This has the effect of the viscoelasticity of the single layer having its greatest affects on the reflection coefficient from its top interface and the interface between the viscoelastic layer and the underlying layer. However, all arrivals from deeper layers are affected in some manner.

The normal incidence trace is computed for reference values of $Q(\omega_R)$ of 1000, 100, 50, 30 and 10. The value of $Q(\omega_R) = 1000$ is a progression towards a nearly elastic layer. The value of $Q(\omega_R) = 10$, which falls below the upper bound of 30 for which the theory is assumed valid, has been included to show that progressively smaller values of $Q(\omega_R)$ behave in a predictable manner even if the theoretical limit of applicability has been passed. The use of $Q = 30$ as a lower bound of applicability may also be questioned. The fact that the high frequency approximation appears to produce reasonable results outside of its region of applicability is not an uncommon occurrence.

The reference frequency is chosen to be the same as the predominant frequency of the source wavelet; in this case, 30Hz. A Gabor wavelet is used and defined as

$$f(t) = \sin[\omega_R(t - t_h)] \exp\left[-\left(\frac{\omega_R(t - t_h)}{\gamma}\right)^2\right] \quad (9)$$

where $\omega_R = 2\pi f_R$ with $f_R = 30\text{Hz}$ and the dimensionless damping factor controlling the side lobes chosen to be $\gamma = 4.0$. The half length in the time domain of this pulse, t_h , is approximately given by $t_h \approx \gamma/(2f_R)$. The time dependence of the wavelet and the frequency spectrum are shown in Figure 3 while the velocity, density – depth structure is given in Figure 4.

The normal incidence synthetic traces for the 5 different values of Q are presented in Figures 5 and 6. As no amplitude scaling of any kind is used, Figure 6 is just Figure 5 with the first arrival removed to allow for better viewing. In Figure 6 the grid lines perpendicular to the time axis have been added to emphasize that no time shift in the arrivals occur at different values of Q . Only P-wave primaries are included in the traces. There are provisions for the introduction of multiples, which has not been implemented for this preliminary presentation. As $Q=1000$ corresponds to the layer approaching the elastic case, conclusions as to the effect of introducing viscoelasticity are left to the reader's observations of variations between the traces with different values of $Q(\omega)$ shown in Figures 5 and 6.

CONCLUSIONS

The use of vertical incidence synthetic seismograms in the exploration of the effects of anelasticity on the surface recorded PP arrivals has been examined. In addition, a special case vertical incidence at an interface between two anelastic halfspaces where the only quantity to vary is the quality factor Q . In the upper medium $Q \rightarrow \infty$, while in the lower halfspace Q is allowed to vary. As would be expected, as Q in the lower medium becomes large ($Q \gg 1$), the reflection coefficient tends to zero. For comparative purposes an AVO plot of the amplitude and phase of the PP acoustic reflection is presented for an elastic halfspace over an anelastic halfspace. Normal incidence PP synthetic seismograms are shown for a plane layered medium with two anelastic layers in the sequence. The synthetics are plotted for a range of values of Q in the two anelastic layers.

REFERENCES

- Aki, K. and Richards. P.G., 1980, Quantitative Seismology, vol. 1, W.H. Freeman and Company, San Francisco.
- Brekhovskikh, L.M., 1980, Waves in Layered Media, Academic Press, New York.
- Daley, P.F., 2003, Short note: Normal incidence synthetics in viscoelastic media, CREWES Report. 15.
- _____, (1981) Seismic Wave Attenuation, Geophysics Reprint Series, Society of Exploration Geophysicists, N.M. Toksöz and D.M. Johnston: Eds.
- Futterman, W.I., (1962), Dispersive body waves, *Journal of Geophysical Research*, 67, 5279-5291.

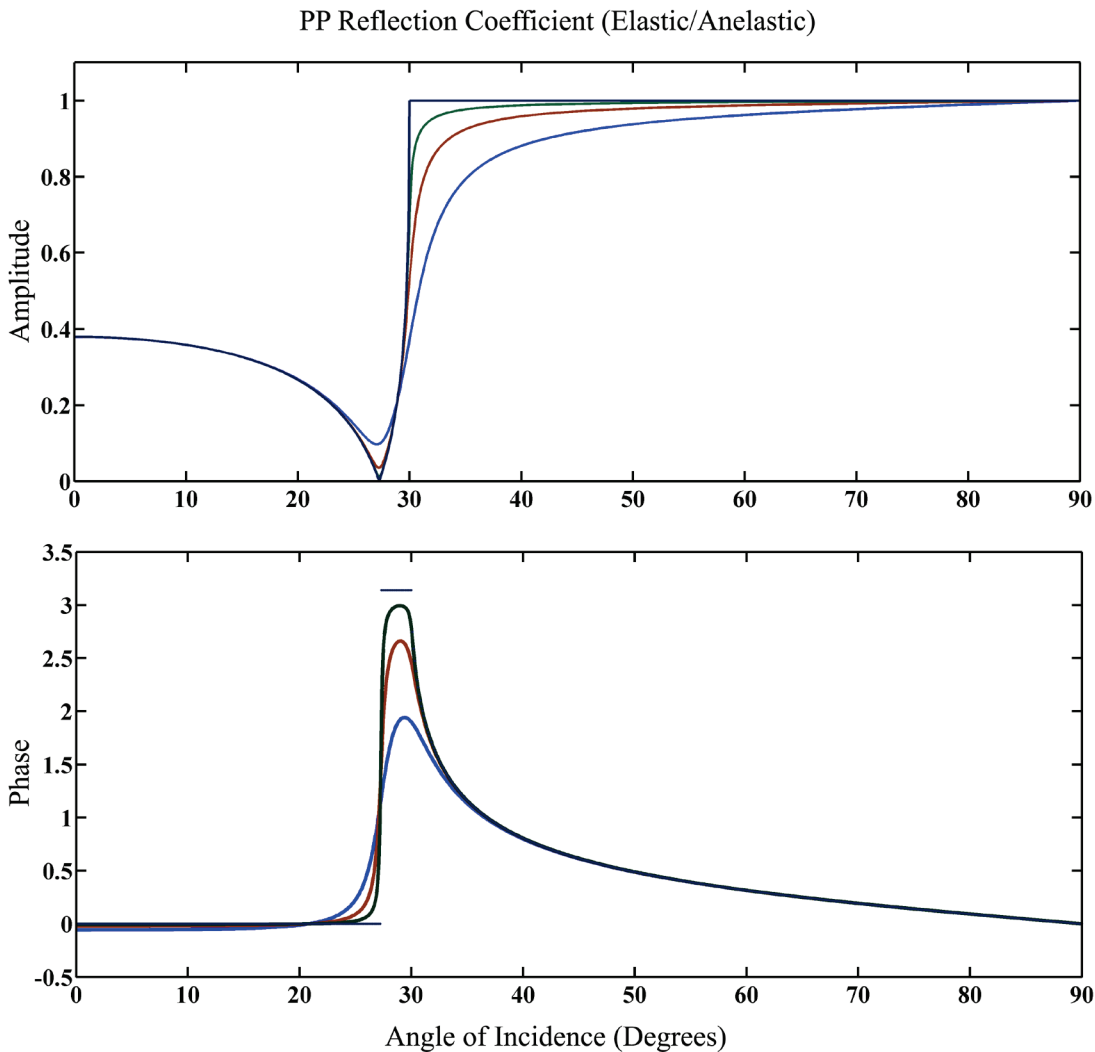


FIG. 1 The general case of PP reflection at the interface between two acoustic anelastic media. The upper medium is assumed to be elastic ($Q \rightarrow \infty$) while Q in the lower medium is plotted (amplitude and phase versus incident angle) for the Q values 10 (blue), 30 (red), 100 (green) and ($Q \rightarrow \infty$) (black). The densities and reference velocities are $(2 \text{ gm/cm}^2, 1000 \text{ m/s} - \text{upper - incident})$ and $(2.1 \text{ gm/cm}^2, 2000 \text{ m/s} - \text{lower})$.

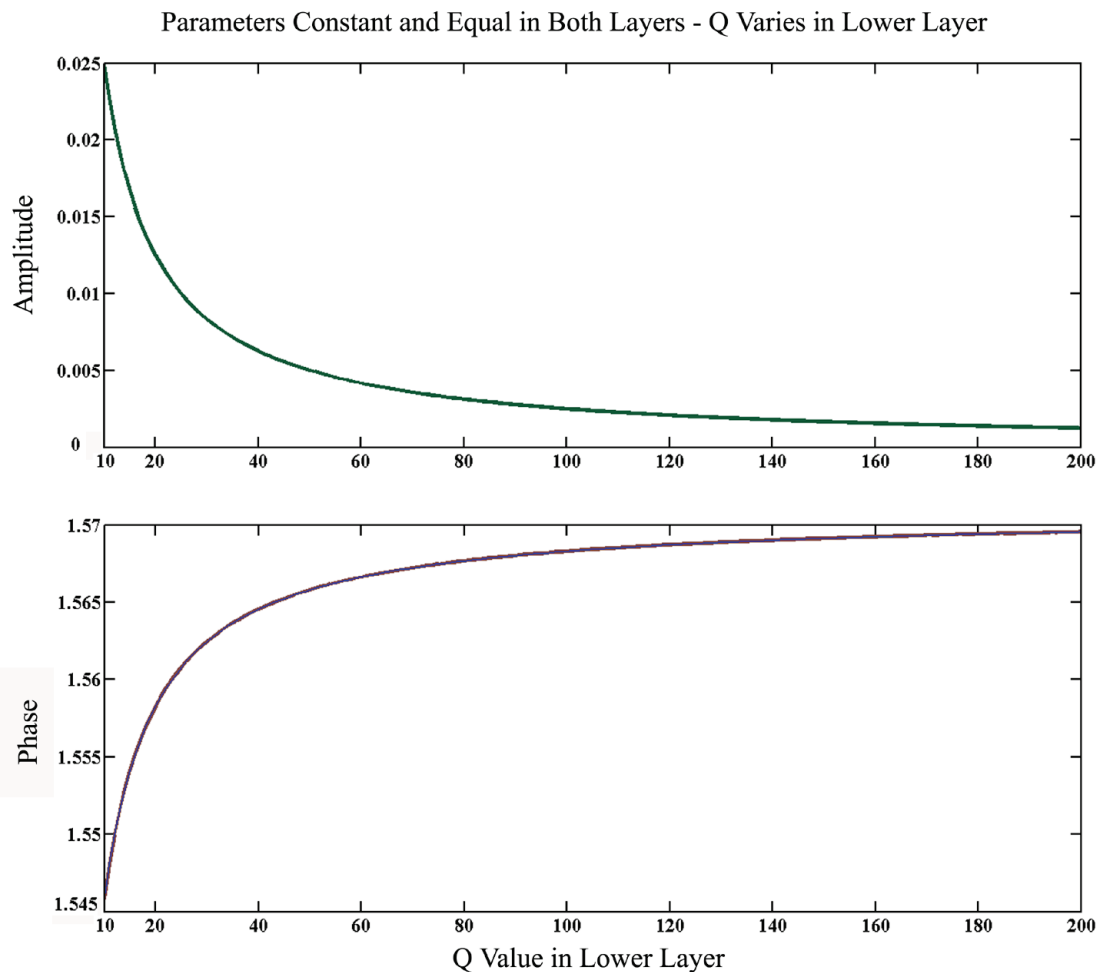


FIG. 2. *PP* reflection from an interface where the only quantity that varies across the interface is Q . The upper (incident) medium is assumed to be elastic ($Q \rightarrow \infty$) while the amplitude and phase of the normal incident reflection coefficient is plotted versus a varying value of Q in the lower medium.

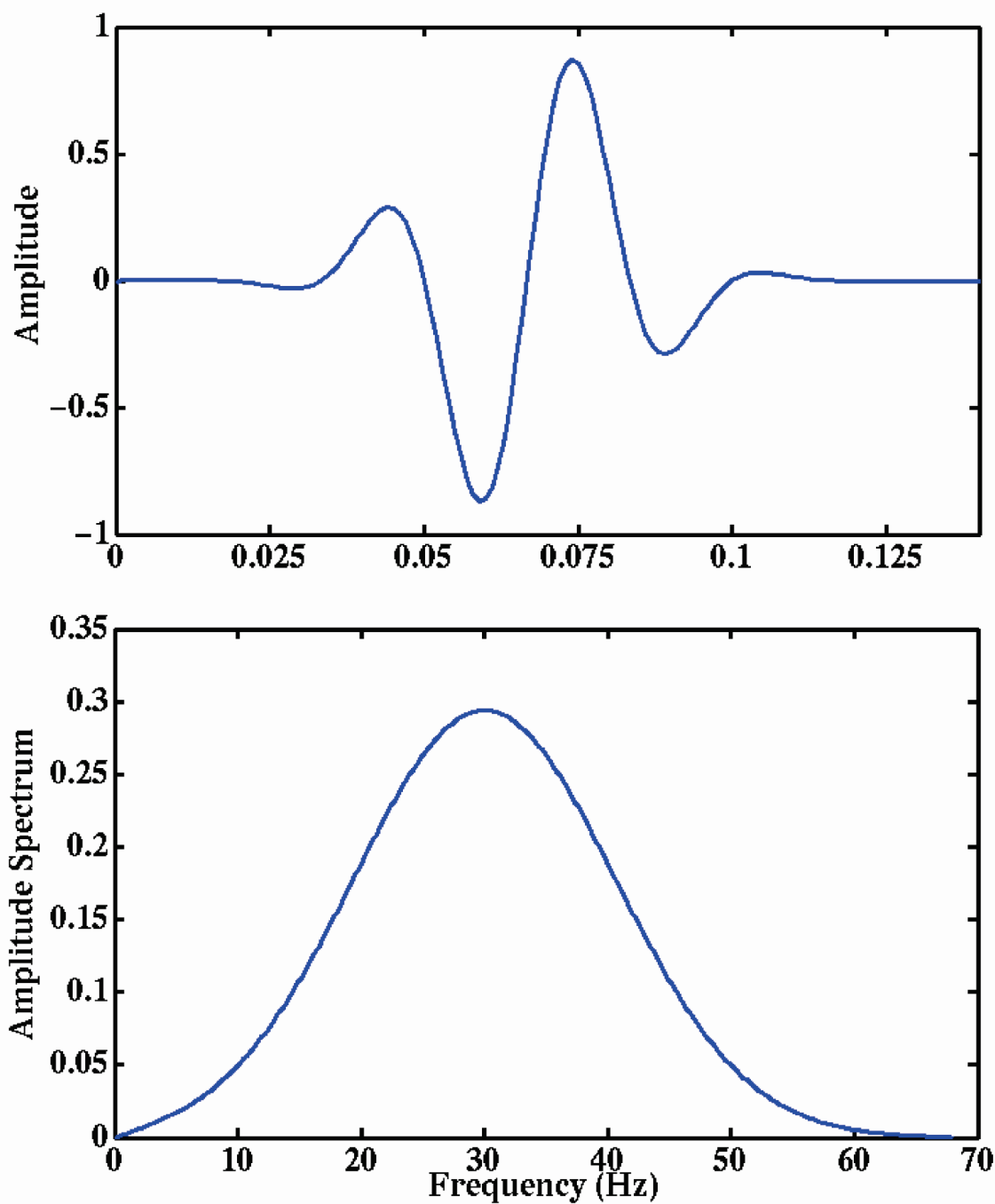


FIG. 3. The time and frequency dependence of the Gabor wavelet with a predominant frequency of 30 Hz and a damping factor of 4.

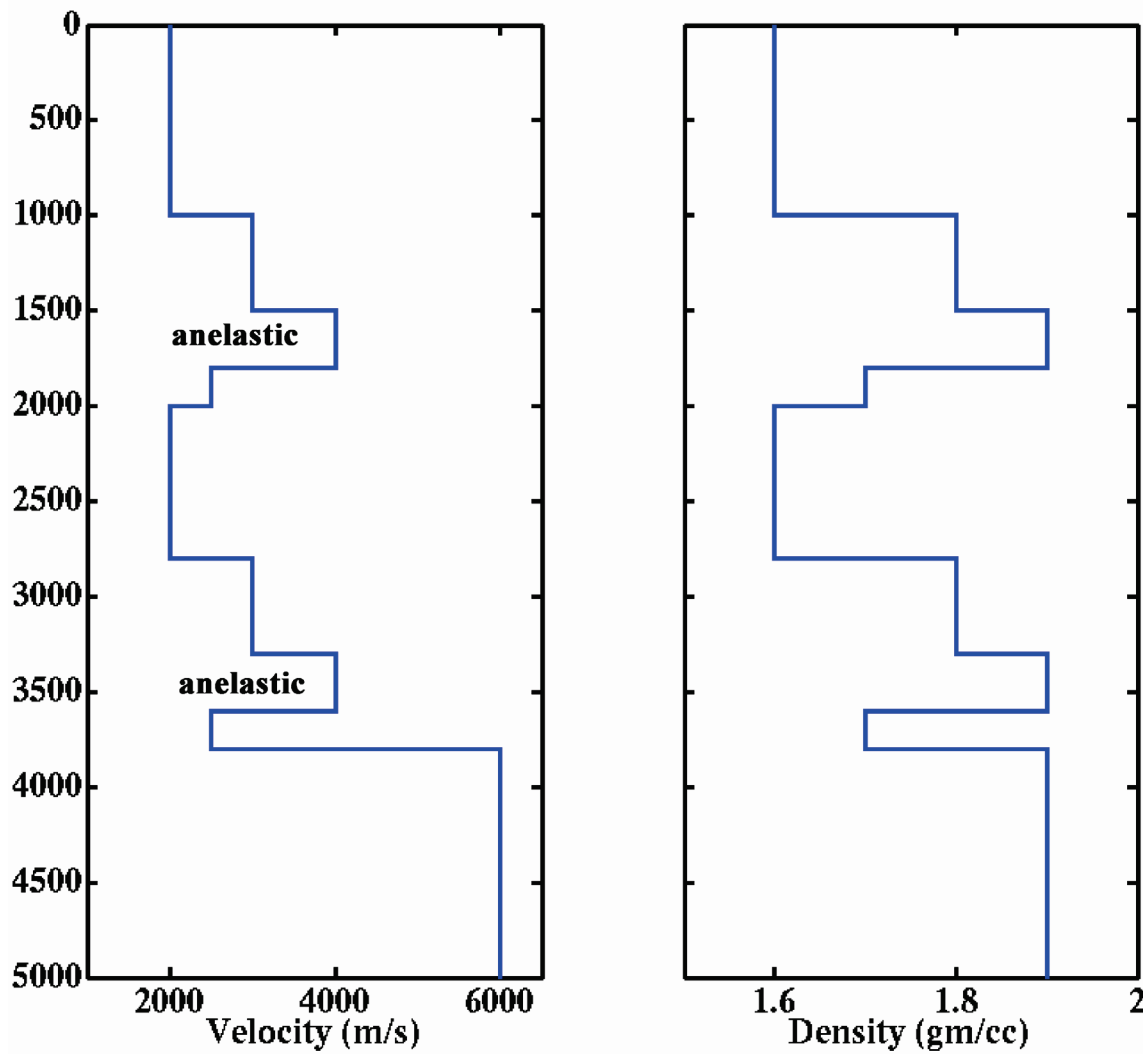


FIG. 4. Velocity and density versus depth profiles for the model considered in this report. The velocities are reference velocities supposedly measured at some reference frequency. In actuality they reflect the velocities that would be measured if the media were elastic. The two anelastic layers are indicated on the velocity depth plot.

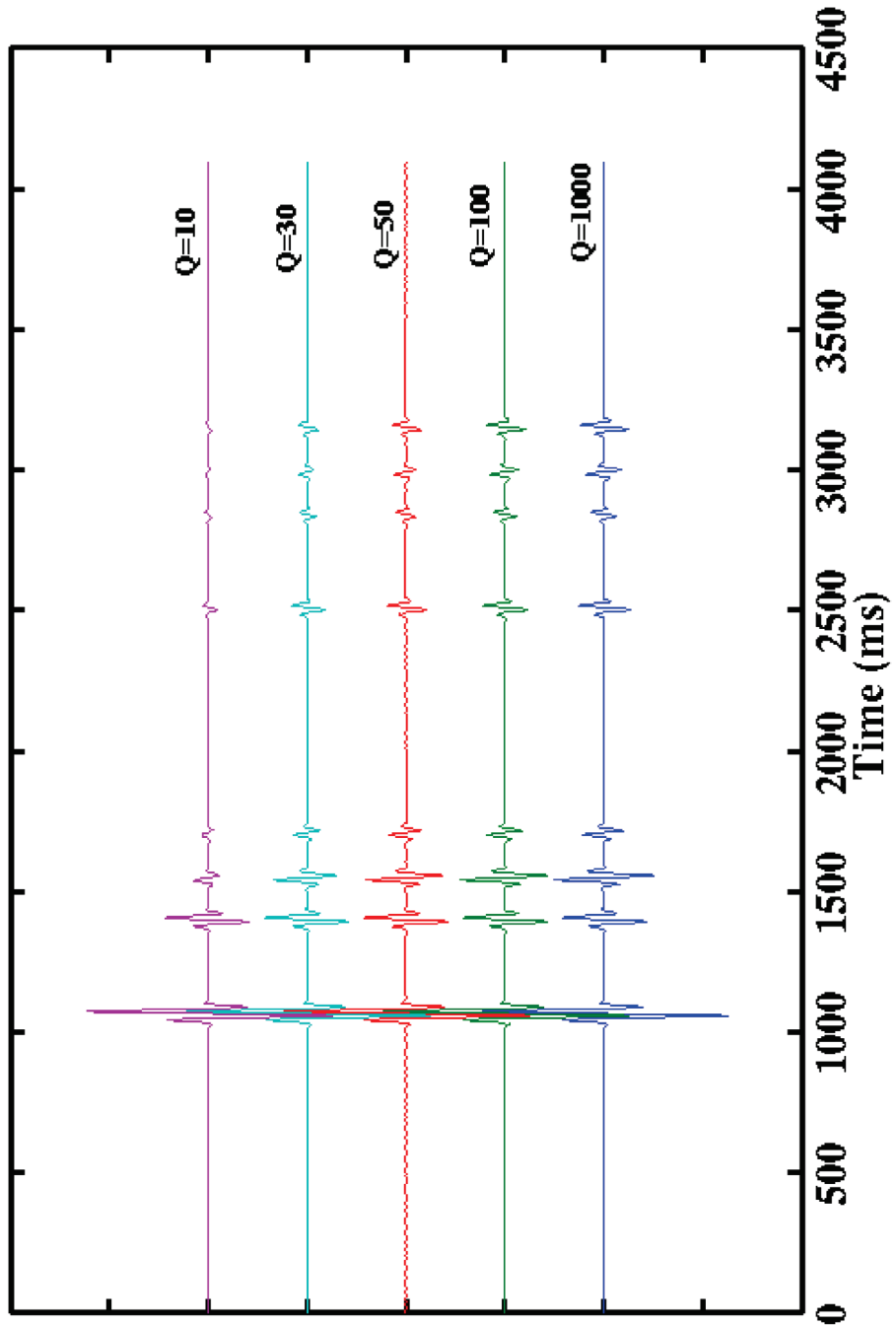


FIG. 5. Normal incidence plots of traces using the model given in Figure 4. Five different reference values of Q are shown. The viscoelastic layers are 3 and 7 and the other layers are constrained to be elastic. This aids in discerning what the effects are of an individual viscoelastic on a synthetic trace.

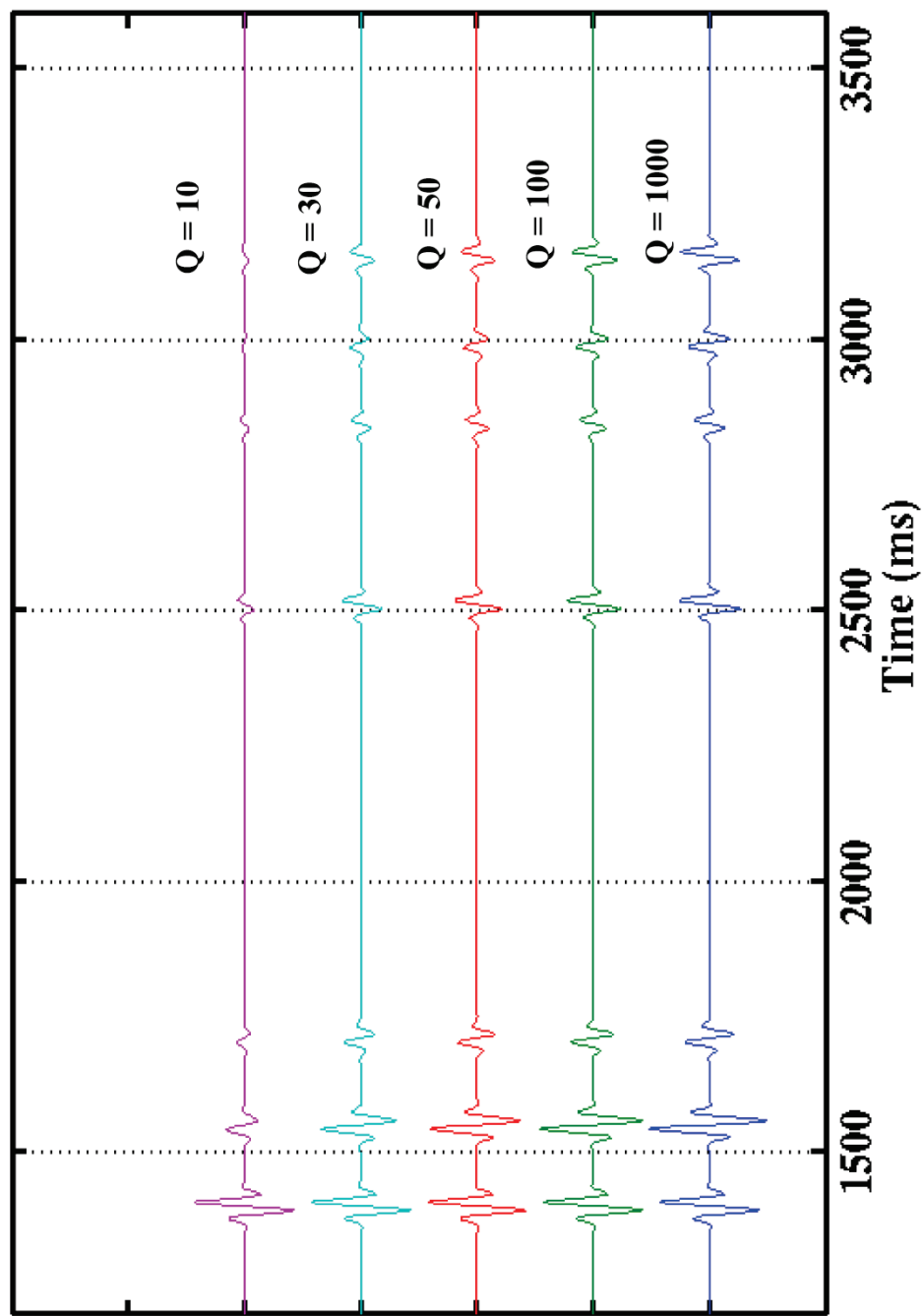


Fig. 6. The same as Figure 5 with the large first primary arrival removed to give a better view of what occurs when anelasticity is introduced into synthetic trace computation. The time grid lines are to indicate that there is no introduction of acausal effects.